

Calcium Entry in Rabbit Corneal Epithelial Cells: Evidence for a Nonvoltage Dependent Pathway

A. Rich, J.L. Rae

Departments of Physiology and Biophysics, and Ophthalmology, Mayo Foundation, Rochester, Minnesota 55905

Received: 8 July 1994/Revised: 11 November 1994

Abstract. We performed experiments to elucidate the calcium influx pathways in freshly dispersed rabbit corneal epithelial cells. Three possible pathways were considered: voltage-gated Ca^{++} channels, $\text{Na}^+/\text{Ca}^{++}$ exchange, and nonvoltage-dependent Ca^{++} -permeable channels. Whole cell inward currents carrying either Ca^{++} or Ba^{++} were not detected using voltage clamp techniques. We also used imaging technology and the Ca^{++} -sensitive ratiometric dye fura 2 to measure changes in intracellular Ca^{++} concentration ($[\text{Ca}]_i$). Bath perfusion with NaCl Ringer's solution containing the calcium channel agonist Bay-K-8644 (1 μM), or Ni^{++} (40 μM), a blocker of many voltage-dependent calcium channels, did not affect $[\text{Ca}^{++}]_i$. Membrane depolarization with a KCl Ringer's bath solution resulted in a decrease in $[\text{Ca}^{++}]_i$. These results are inconsistent with the presence of voltage gated Ca^{++} channels. Nonvoltage gated Ca^{++} entry, on the other hand, would be reduced by membrane depolarization and enhanced by membrane hyperpolarization. Agents which hyperpolarize via stimulation of K^+ current, such as flufenamic acid, resulted in an increase in ratio intensity. The cells were found to be permeable to Mn^{++} and bath perfusion with 5 mM Ni^{++} decreased $[\text{Ca}^{++}]_i$ suggesting that the Ca^{++} conductance was blocked. These results are most consistent with a nonvoltage gated Ca^{++} influx pathway. Finally, replacing extracellular Na^+ with Li^+ resulted in an increase in $[\text{Ca}^{++}]_i$ if the cells were first Na^+ -loaded using the Na^+ ionophore monensin and ouabain, a $\text{Na}^+/\text{K}^+/\text{ATPase}$ inhibitor. These results suggest that $\text{Na}^+/\text{Ca}^{++}$ exchange may also regulate $[\text{Ca}^{++}]_i$ in this cell type.

Key words: Fura 2 — Fluorescent imaging — Cornea — Epithelia — Calcium conductance

Introduction

Calcium plays an important role in the regulation of a variety of cellular functions including excitation-contraction in muscle cells, stimulus-secretion coupling in nerve and neuroendocrine cells, and acts as a second messenger for many signal transduction pathways. As a signaling ion, levels of free calcium directly regulate the activity of intracellular enzymes, such as protein phosphatases and kinases. Intracellular calcium concentration may also modulate the ionic conductance of the plasma membrane either directly, as in calcium activated potassium channels, or indirectly through second messenger pathways. Some of these regulatory actions have been observed in ocular epithelia. For example, in rabbit corneal epithelium extracellular calcium has been shown to be required for activation of a potassium current by cGMP (Farrugia & Rae, 1992), increases in intracellular calcium cause a partial block of one type of potassium channel (Rae et al., 1990b), and calcium stimulates a nonselective cation channel in the rabbit corneal endothelium (Rae et al., 1990a). Calcium has also been shown to act as a second messenger for adrenergic receptor-mediated responses in bovine corneal epithelial cells (Reinach et al., 1992).

Intracellular calcium concentration ($[\text{Ca}^{++}]_i$) is tightly regulated at levels that are 1,000 to 100,000 times lower than the extracellular $[\text{Ca}^{++}]_o$. The steady-state electrochemical gradient for calcium is maintained by Ca-ATPase pumps located on the endoplasmic reticulum (ER) and the plasma membrane. The presence of this type of transporter has been verified in the plasma membrane of bovine corneal epithelium (Reinach, Holmberg & Chiesa, 1991). Other mechanisms, such as $\text{Na}^+/\text{Ca}^{++}$ exchange, utilize the Na^+ electrochemical gradient to maintain low intracellular $[\text{Ca}^{++}]_i$. Short term regulation of intracellular $[\text{Ca}^{++}]_i$ can also be modulated by Na^+ -

Ca^{++} exchange. For example, during the upstroke and plateau phase of the cardiac action potential, Na^+ - Ca^{++} exchange operates in reverse mode and allows Ca^{++} influx (Schulze et al., 1993). Hence Na^+ - Ca^{++} exchange may contribute to an increase in cell calcium on a short time scale, or it can mediate Ca^{++} efflux in the steady state. The contribution of Na^+ - Ca^{++} exchange to intracellular $[\text{Ca}^{++}]$ will be determined by the transcellular Na^+ and Ca^{++} gradients, and the membrane potential.

Steady-state intracellular $[\text{Ca}^{++}]$ will be determined by the balance between calcium influx and efflux across the plasma membrane, and by intracellular calcium buffering mechanisms including calcium binding proteins or sequestration by organelles such as the endoplasmic reticulum and mitochondria. The focus here is on Ca^{++} entry. Several calcium entry mechanisms have recently been identified in nonexcitable cells. Depletion of intracellular Ca^{++} stores stimulates Ca^{++} entry and leads to elevated intracellular $[\text{Ca}^{++}]$ (Fasolato, Innocenti & Pozzan, 1994). Hoth and Penner first described the molecular basis for this inward calcium-selective current in mast cells and called it I_{crac} for calcium-release activated calcium current (Hoth & Penner, 1992). This type of current that is activated upon depletion of intracellular Ca^{++} stores has since been identified in several cell types. A different nonvoltage dependent calcium conductance has been identified in endothelial cells (Luckhoff & Clapham, 1992). This current is carried by a 2.5 pS channel that is highly Ca^{++} -selective and, unlike I_{crac} , it is permeable to Mn^{++} and Ba^{++} and is directly activated by IP_4 (inositol 1,3,4,5-tetrakisphosphate).

The mechanisms that control the intracellular calcium concentration in the rabbit corneal epithelium are currently unknown. Calcium selective entry pathways may be divided into three major classes: (i) voltage-gated ion channels including classical L-type dihydropyridine-sensitive channels, ω -conotoxin sensitive N-type channels, and ω -agatoxin-sensitive P-type channels, (ii) exchange mechanisms such as Na^+ - Ca^{++} exchange, and (iii) nonvoltage-dependent calcium selective channels. These studies were designed to determine whether each of these pathways contributes to calcium influx in rabbit corneal epithelial cells. We have used patch clamp methodology and standard imaging technology with the calcium-sensitive dye fura 2 to determine the calcium influx pathways in freshly dispersed rabbit corneal epithelial cells. The data show that intracellular $[\text{Ca}^{++}]$ increases during maneuvers which hyperpolarize the resting membrane potential, and intracellular $[\text{Ca}^{++}]$ decreases during maneuvers that depolarize the resting membrane potential. These results suggest that the primary calcium entry pathway is via a nonvoltage dependent calcium influx pathway. The data also show that Na^+ - Ca^{++} exchange mechanisms may contribute to calcium influx.

Materials and Methods

Adult New Zealand white rabbits with an average weight between 2.5 and 3.0 kg were handled according to the Association for Research in Vision and Ophthalmology (ARVO) guidelines for the use of experimental animals in eye research. The rabbits were euthanized with an overdose of sodium pentobarbital injected into a marginal ear vein.

After removal of the globe, the cornea was cut along the limbus and dissected. The endothelium and Descemet's membrane were removed and the remaining epithelium and stroma were placed in 5 ml of 2.4 units/ml dispase and incubated for approximately 90 min at 37°C. The epithelial sheet was then gently dissected free of the stroma and placed in 10 ml of calcium-free Ringer's solution containing 0.1% trypsin. Cells were dispersed using gentle trituration at room temperature for 7 min using a programmable tissue agitator (N.B. Datyner, Wellesley Hills, MA). The cell suspension was centrifuged at $180 \times g$ for 7 min and resuspended in enzyme-free Ringer's solution. Centrifugation was repeated and the cells were finally resuspended in a Ringer's solution containing 5 mM glucose and stored on ice. Experiments were performed during the next 6 hr.

Fura 2 AM ester (Molecular Probes) was dissolved in dimethyl sulfoxide (DMSO) and mixed with an equal volume of a 20% wt/vol Pluronic F-127:DMSO mixture resulting in a 1 mM stock solution. Freshly dispersed rabbit corneal epithelial cells were dye-loaded with fura 2 at room temperature in a NaCl Ringer's solution containing 1 μM fura 2 AM for 7–10 min, centrifuged for 7 min at $180 \times g$, and resuspended in a dye-free NaCl Ringer's solution. Initial experiments included a 30 min incubation period at 35°C to ensure complete hydrolysis of the dye-ester chemical bond. However, this did not improve the calcium sensitivity of the measurements and the cells appeared to be less viable, so this procedure was discontinued. Several drops of the cell suspension were placed in a glass-bottomed recording chamber containing NaCl Ringer's solution and allowed to settle and adhere to the bottom for 40 min. Firmly attached single cells with good fluorescence emission were selected for experiments.

The chambers were perfused continuously with NaCl Ringer's solution containing (in mM): 4.74 KCl, 149.2 NaCl, 2.54 CaCl_2 , and 5 HEPES resulting in a final osmolarity of 293 mosmol/kg. KCl was substituted for NaCl in KCl Ringer solution. All solutions were adjusted to a final pH of 7.35. The chamber volume was approximately 0.5 ml and the bath perfusion rate was 2.1 ml/min so that complete turnover of bath contents, taken as a 5 \times volume change, was approximately 1.2 min. Ouabain and monensin (Sigma Chemical, St. Louis, MO) were dissolved in NaCl Ringer and ethanol, respectively, as 10 mM stock solutions. Ionomycin was dissolved in ethanol as a 10 mM stock solution. Bay K 8644 was dissolved in ethanol as a 2 mM stock solution. Stock solutions were stored frozen and diluted to the desired concentration for each experiment.

Dye loaded cells were observed with a Nikon Diaphot epifluorescence microscope using a 40 \times (0.85 NA) oil immersion objective. Experiments were performed at room temperature. The light from a 75 Watt xenon lamp was bandpass-filtered at 340 nm or 380 nm (15 nm bandwidth, Omega Optical, Brattleboro, Vermont) using a computer-controlled filter wheel (Alantex + Zieler Instrument Corp.). A quartz fiber optic scrambler was used to deliver a focused, homogeneous light source to the dichroic mirror (Nikon DM 400). Fluorescence emission was filtered at 510 nm and detected with a Hamamatsu CCD camera. A Hamamatsu C2400 CCD camera controller and high voltage intensifier controller were used to adjust the camera gain, offset, and sensitivity for each experiment to maximize the signal intensity. Background images were collected before each experiment to account for the dark current at the camera. Shading corrections were obtained by taking images of calcium-saturated fura 2 to account for irregularities

in the light intensity at the experimental field. Images were captured after excitation at each wavelength every 15 sec for most experiments. The coordination of the shutters, light illumination, and subsequent data acquisition were controlled by Universal Imaging hardware and Image-1/FL software run on an Intel 80486 based microcomputer. Images at each excitation wavelength were stored on a Bernoulli cartridge for later data analysis. The stored images consisted of a 512 × 512 array and fluorescence intensity was collected on an 8-bit scale. The fluorescence intensity values are the average value (zero intensity values were excluded from the average) for a region that was drawn around each cell.

Free calcium concentration may be calculated from the equation:

$$[Ca^{++}] = K_d^{fura\ 2} \cdot \beta \frac{R - R_{min}}{R_{max} - R} \quad (1)$$

where R is the 340 nm/380 nm ratio, R_{max} is the ratio when the dye is saturated with calcium, R_{min} is the ratio at zero free calcium, β is the 380 nm signal of fura 2 at very low free calcium divided by the 380 nm signal at saturating calcium, and $K_d^{fura\ 2}$ is the dissociation constant of fura 2 for calcium (Grynkiewicz, Poenie & Tsien, 1985). The β value depends upon the camera gain, among other things unique to each experimental setup, and must be determined for each experiment. $K_d^{fura\ 2}$ will vary with pH, temperature, viscosity, and ionic strength and therefore must be determined for the intracellular environment. A series of solutions with precisely controlled free $[Ca^{++}]$ are necessary to determine the $K_d^{fura\ 2}$. Therefore the total amount of EGTA in the solutions must be determined. The purity of our EGTA (Sigma, lot 120H5605) was measured using a potentiometric technique and found to be 93% (Marks & Maxfield, 1991). We used a reciprocal-dilution method to prepare a series of NaCl Ringer's solutions with free $[Ca^{++}]$ ranging from 17 nM to 75 μ M. These solutions resulted in a $K_d^{fura\ 2}$ (free acid form) of 97 nM and a β value of 1.9 on the imaging setup.

The second major step is to completely equilibrate intracellular $[Ca^{++}]$ with bath $[Ca^{++}]$ in fura 2 loaded cells for several different concentration values. Initial attempts were made using the Na⁺ ionophore monensin (5 μ M), the K⁺ ionophore nigericin (5 μ M), and the calcium ionophore ionomycin (5 μ M). Under these conditions, no change in intracellular $[Ca^{++}]$ was measured until bath $[Ca^{++}]$ was increased above 1 μ M. Increasing the $[Ca^{++}]$ in the bath to 2.54 mM from 40 μ M resulted in a further increase in the fluorescence ratio. Since the $K_d^{fura\ 2}$ is reported to be 135 nM at pH 7.1–7.2 and 20°C (Grynkiewicz, Poenie & Tsien, 1985) the cells were clearly not equilibrated with the bath $[Ca^{++}]$. For this reason, and because we were not able to measure a β value in each experiment, we report the fluorescent intensity values rather than concentration values. We do report the $[Ca^{++}]$ values for the first figure using the appropriate $K_d^{fura\ 2}$ taken from the literature to allow comparison with values reported from other tissues.

Patch electrodes for whole-cell recordings were made from Kimble KG-12 glass (Garner Glass, Claremont, CA) and pulled on a Sutter Instruments (Novato, CA) P-80 microelectrode puller. Tips were coated with Dow Corning (Midland, MI) sylgard #184 and fire polished under direct observation to a final resistance of 3–5 M Ω . Whole-cell recordings were made using the amphotericin-perforated patch technique as previously described (Rae et al. 1991). The electrodes were mounted in a polycarbonate holder connected to an Axopatch 200 patch voltage clamp amplifier (Axon Instruments, Foster City, CA) and positioned immediately adjacent to the cell membrane. Slight suction resulted in a gigohm seal for the majority of cells. Amphotericin usually partitioned into the membrane isolated in the membrane tip within 15 min, resulting in a stable access resistance ranging from 9 to 20 M Ω . Data were recorded using a modified IBM-AT computer using a TL-1

Labmaster interface (Axon Instruments) and driven by PClamp software (Version 5.6, Axon Instruments) allowing voltage clamp protocols with concomitant digitization of the membrane currents. Whole-cell current records were collected at 2 kHz and filtered at 1 kHz with a 4-pole Bessel filter. Voltage step protocols were repeated five times and the resulting currents at each voltage were averaged to produce the final records. All of the current-voltage relationships were corrected for the offset potential by subtracting 10 mV. Capacity transients were adjusted during recording. Records were not leak-subtracted since it was not possible in each cell to determine whether a nonvoltage dependent current that reversed at 0 mV resulted from nonspecific leak (i.e., from the glass-membrane interface) or was mediated by a physiological leak pathway, such as the nonspecific cation conductance that would also reverse at 0 mV. Data were analyzed using PClamp software (Axon Instruments, Foster City, CA) or using custom written macros in Excel (Microsoft, Redman, WA). Final plots were prepared using SigmaPlot (Jandel, Madera, CA).

Results

Voltage-dependent calcium permeable channels are activated by membrane depolarization. A series of whole-cell voltage clamp experiments using the amphotericin perforated patch technique and a voltage step protocol with a holding potential of –70 mV and 300 msec depolarizing steps from –90 to +50 mV was used to assay this calcium entry pathway. Attempts to enhance inward current magnitude included using either 80 mM Ba⁺⁺ or Ca⁺⁺ in the bath solution, stimulation with the dihydropyridine agonist Bay K 8644, and elevated temperature. No inward current was detected (*data not shown*).

The possibility remains that a very small inward current, undetectable by voltage clamp methodology, contributes to calcium influx. Therefore fluorescence ratio experiments were performed. If voltage-gated calcium channels are present then membrane depolarization would be expected to result in an increase in calcium influx and thereby increase intracellular $[Ca^{++}]$. The effects of replacing external Na⁺ with K⁺ are shown in Fig. 1. The top panel shows the 340 nm/380 nm ratio that is proportional to intracellular $[Ca^{++}]$. Membrane depolarization was accompanied by a decrease in the 340 nm/380 nm ratio, just the opposite from what would be expected in the presence of voltage-gated calcium channels. The single wavelength intensities, shown in the middle panel, verify that the ratio changes were in fact due to a decrease in the 340 nm intensity and an increase in the 380 nm intensity, as expected from a decrease in intracellular $[Ca^{++}]$. The bottom panel shows an estimate of intracellular $[Ca^{++}]$ calculated using Eq. 1. Cells were permeabilized with ionomycin (10 μ M) to clamp intracellular $[Ca^{++}]$ with bath $[Ca^{++}]$. As discussed in Materials and Methods, a reliable value for the K_d for fura 2 has not been determined in this preparation and a K_d value corresponding to the experimental conditions (135 nM, pH 7.1–7.2, 20°C) was therefore selected from the literature (Grynkiewicz, Poenie & Tsien, 1985).

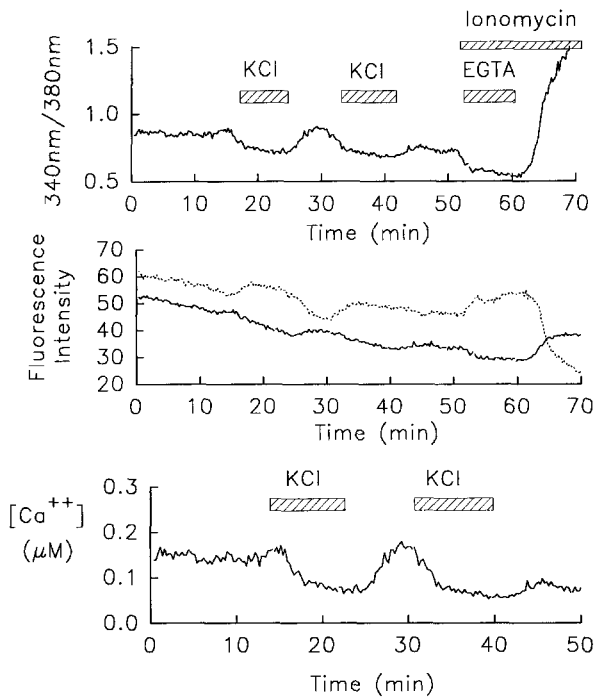


Fig. 1. Effects of KCl-induced membrane depolarization on intracellular $[Ca^{++}]$. The bath solution is NaCl Ringer unless otherwise noted. The top panel shows the 340 nm/380 nm ratio, proportional to intracellular $[Ca^{++}]$. Depolarization of the resting membrane potential with KCl resulted in a decrease in the ratio and the effects were reversible upon membrane repolarization with NaCl. The middle panel shows the effects on the single wavelength fluorescence intensity. Increases in the ratio are caused by an increase in the 340 nm intensity (continuous line) and a decrease in the 380 nm intensity (broken line) indicating that changes in the ratio are in fact due to alterations in the ratio of $[Ca:fura\ 2]/[fura\ 2]$. The bottom panel shows the calculated $[Ca^{++}]$ using Eq. 1.

Voltage-dependent calcium currents are known to inactivate in a time and voltage-dependent manner. A very small inward Ca^{++} current could rapidly inactivate and therefore not contribute significantly to intracellular $[Ca^{++}]$. Bay K 8644, a dihydropyridine calcium channel agonist, prolongs channel openings and thereby increases the steady state inward calcium current. The effects of bath perfusion with Bay K 8644 ($10\ \mu M$) are shown in Fig. 2. The top panel shows the 340 nm/380 nm ratio and the bottom panel shows the single wavelength intensities. Application of Bay K 8644 in NaCl Ringer solution had no effect on the fluorescence ratio. The bath was subsequently perfused with KCl Ringer in the continued presence of Bay K 8644 to depolarize the membrane and therefore further increase the open probability of voltage-gated calcium channels. Under these conditions the intracellular $[Ca^{++}]$ decreased, contrary to what would be expected in the presence of dihydropyridine-sensitive channels. Voltage-gated calcium channels are also known to be inhibited by low concentrations of Ni^{++} . Bath perfusion with Ni^{++} ($40\ \mu M$) had no effect on

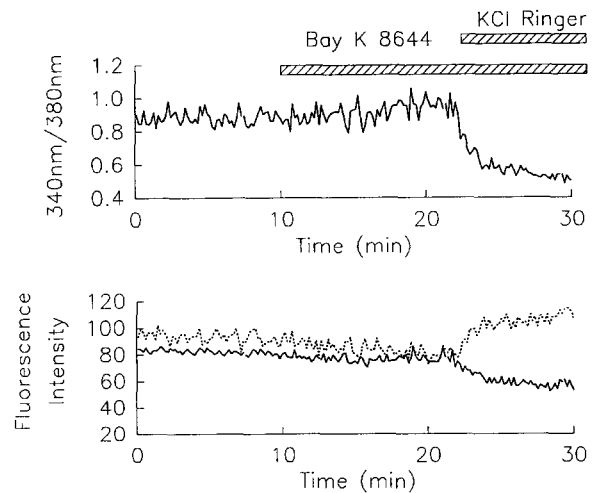


Fig. 2. Bath perfusion with the calcium channel agonist Bay K 8644 ($10\ \mu M$) had no effect on intracellular $[Ca^{++}]$ during perfusion with NaCl Ringer's solution. Membrane depolarization with elevated KCl, in the presence of Bay K 8644, resulted in a decrease in intracellular $[Ca^{++}]$. The top panel shows the 340 nm/380 nm ratio, proportional to $[Ca^{++}]$, and the bottom panel shows the 340 nm (continuous line) and the 380 nm (broken line) intensities.

the fluorescence ratio ($n = 3$, *data not shown*). These data suggest that voltage-gated calcium channels do not contribute to Ca^{++} influx.

Sodium calcium exchange mechanisms use the inward-directed Na^{+} electrochemical gradient to drive Ca^{++} out of the cell, against its electrochemical gradient to maintain a low intracellular $[Ca^{++}]$. However, the exchanger can also operate in reverse mode under some conditions, and thereby allow calcium influx and Na^{+} efflux. Decreasing $[Na^{+}]$ in the bath solution would be expected to result in Na^{+} efflux and Ca^{++} influx by the Na^{+} - Ca^{++} exchanger, and therefore increase intracellular $[Ca^{++}]$. However, replacing extracellular Na^{+} with K^{+} resulted in a decrease in intracellular $[Ca^{++}]$ (see Fig. 1 and 2). These results suggest that Na^{+} - Ca^{++} exchange may not be the primary regulator of intracellular $[Ca^{++}]$ under these experimental conditions.

If intracellular Na^{+} is clamped at a low level by Na^{+} - K^{+} ATPase then extracellular $[Na^{+}]$ reduction may not be sufficient to reverse the transport direction of Na^{+} - Ca^{++} exchange (Sage, van Breeman & Cannel, 1991). Therefore, experiments were designed to increase intracellular $[Na^{+}]$ which would be expected to result in an increase in Ca^{++} influx if Na^{+} - Ca^{++} exchange is present. Figure 3 shows the fluorescence ratio during application of $10\ \mu M$ ouabain, expected to block Na^{+} - K^{+} -ATPase, followed by the application of $10\ \mu M$ monensin, a Na^{+} ionophore. Little or no change was observed in the fluorescence ratio under these conditions. Replacement of extracellular Na^{+} with Li^{+} was accompanied by a rise in the fluorescence ratio indicating an increase in intra-

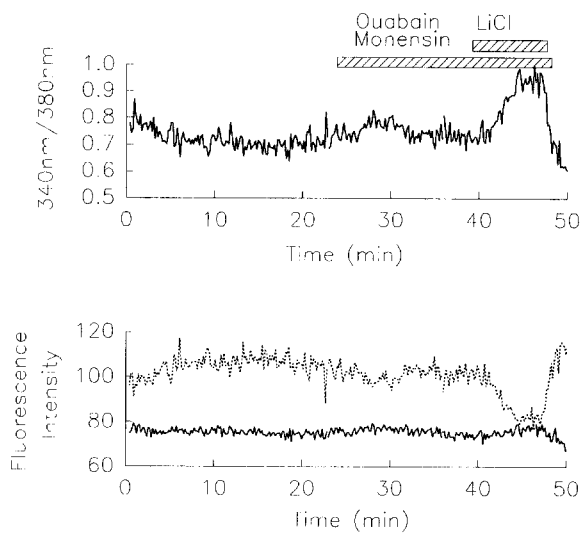


Fig. 3. Effects of the Na-K-ATPase inhibitor ouabain ($10 \mu\text{M}$) and the Na^+ ionophore monensin ($10 \mu\text{M}$) on intracellular $[\text{Ca}^{++}]$. The top panel shows the 340 nm/380 nm ratio and the bottom panel shows the 340 nm (continuous line) and the 380 nm (broken line) intensities.

cellular $[\text{Ca}^{++}]$. This effect was observed in six out of nine experiments. These results are consistent with an internal- Na^+ dependent Ca^{++} transport mechanism.

The decrease in intracellular $[\text{Ca}^{++}]$ when extracellular Na^+ is replaced with K^+ cannot be explained by either voltage-gated calcium channels or by Na^+ - Ca^{++} exchange mechanisms. Calcium entry via nonvoltage-gated calcium channels would be modulated, in part, by the driving force for calcium entry. Replacing extracellular Na^+ with K^+ will depolarize the resting membrane potential and reduce the driving force for calcium entry. If a nonvoltage-gated calcium entry pathway modulates Ca^{++} influx then decreasing the driving force for Ca^{++} entry would result in a decrease in intracellular $[\text{Ca}^{++}]$. The results shown in Fig. 1 are consistent with this type of mechanism. Conversely, membrane hyperpolarization would increase the driving force for Ca^{++} entry and would be predicted to increase Ca^{++} influx. This hypothesis was tested using flufenamic acid which has been shown to stimulate outward K^+ current (I_{K}) and hyperpolarize the resting membrane potential (Rae & Farrugia, 1992). The effects of flufenamic acid ($200 \mu\text{M}$) on the fluorescence ratio are shown in Fig. 4. Perfusion with flufenamic acid in EGTA-buffered NaCl Ringer's solution has no effect on intracellular $[\text{Ca}^{++}]$. However, intracellular $[\text{Ca}^{++}]$ rapidly increases when Ca^{++} is returned to the bath solution. Similar results were obtained in sixteen experiments. These results suggest that membrane hyperpolarization with flufenamic acid increases intracellular $[\text{Ca}^{++}]$ and that extracellular calcium is necessary for this response.

Since stimulation of I_{K} with cGMP requires the presence of calcium in the bath solution (Farrugia & Rae,

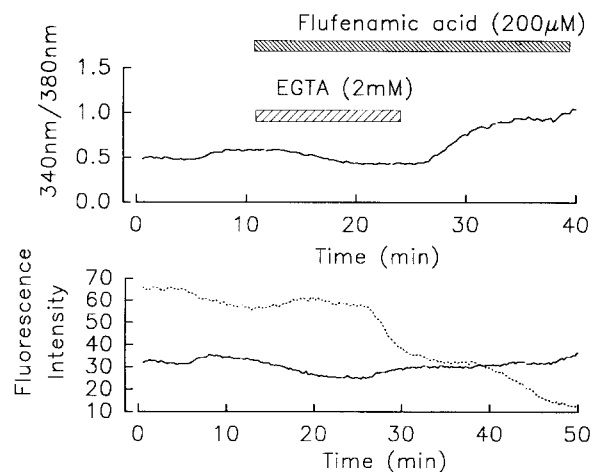


Fig. 4. Effects of flufenamic acid on intracellular $[\text{Ca}^{++}]$ in calcium free and normal calcium bath solutions. The top panel shows that flufenamic acid in low calcium ($2 \text{ mM EGTA} \approx \text{nM } [\text{Ca}^{++}]$) does not alter the ratio. Calcium addition to the bath solution, in the presence of flufenamic acid, results in a large increase in the ratio. The bottom panel shows the 340 nm (continuous line) and the 380 nm (broken line) intensities.

1992) it is possible that flufenamic acid also requires extracellular calcium to stimulate I_{K} and hyperpolarize E_{m} . Therefore, the effects of flufenamic acid on I_{K} in Ca^{++} -free solution were measured. The cell membrane potential was held at -70 mV and stepped from -100 to $+90 \text{ mV}$ in 10 mV increments for 250 msec , returning to -70 mV between steps. Figure 5 shows whole cell currents measured in NaCl Ringer's solution containing 2 mM EGTA (A), and after stimulation with $100 \mu\text{M}$ flufenamic acid in calcium free solution (B). Flufenamic acid clearly stimulates I_{K} in the absence of extracellular calcium. However, re-addition of Ca^{++} to the bath solution (C) also increased I_{K} . The current-voltage relationship for this experiment is shown in D. Bath perfusion with $100 \mu\text{M}$ flufenamic acid in calcium-free solution resulted in a membrane hyperpolarization from -50 ± 6 (SEM, $n = 9$) to $-58 \pm 5 \text{ mV}$ and an increase in I_{K} from 551 ± 178 to $838 \pm 199 \text{ pA}$. Subsequent perfusion with normal Ringer's solution (2.54 mM Ca^{++}) in the presence of $100 \mu\text{M}$ flufenamic acid hyperpolarized E_{m} to $-68 \pm 8 \text{ mV}$ and increased I_{K} to $1140 \pm 305 \text{ pA}$. These results suggest that flufenamic acid can stimulate I_{K} in the absence of extracellular Ca^{++} but the effects are potentiated by extracellular Ca^{++} .

Several types of calcium channels, including nonvoltage-gated calcium channels, are inhibited by Ni^{++} . However, nonvoltage-gated calcium channels require relatively high doses ($\geq 10^{-3} \text{ M}$) for block, compared to voltage-gated calcium channels (Luckhoff & Clapham, 1992). The effects of bath perfusion with 5 mM Ni^{++} on the fluorescence ratio are shown in Fig. 6. Application of Ni^{++} resulted in a decrease in the fluorescence ratio,

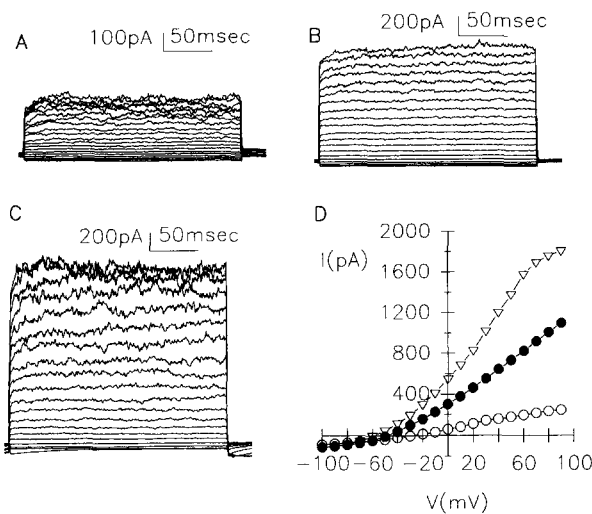


Fig. 5. Effects of flufenamic acid on I_K in Ca^{++} -free solution. (A) shows control currents measured in Ca^{++} -free Ringer's solution containing 2 mM EGTA, (B) shows currents after stimulation with flufenamic acid, and (C) shows the whole cell currents after bath perfusion with normal Ringer's solution containing flufenamic acid. Steady-state currents are plotted versus command potential in (D). Open circles represent control records, filled circles represent stimulation with flufenamic acid in Ca^{++} -free Ringer's solution, and open triangles are the steady-state currents following Ca^{++} addition in the presence of flufenamic acid.

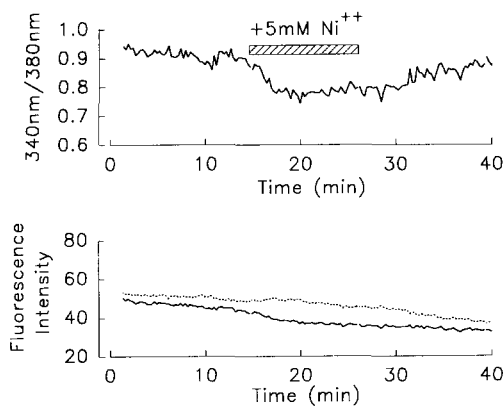


Fig. 6. Bath perfusion with 5 mM Ni^{++} in NaCl Ringer solution resulted in a decrease in the fluorescence ratio (top panel). These data indicate that Ni^{++} inhibits calcium influx. The bottom panel shows that the decrease in the fluorescence ratio results from an increase in the 380 nm (broken line), and a decrease in the 340 nm (solid line), fluorescence intensity.

consistent with an inhibition of Ca^{++} entry across the plasma membrane.

Some nonvoltage-gated Ca^{++} channels are permeable to Mn^{++} , like that described in endothelial cells (Luckhoff & Clapham, 1992), but other nonvoltage-gated conductances, like that described in mast cells (Hoth & Penner, 1992), are not. If the calcium entry pathway in

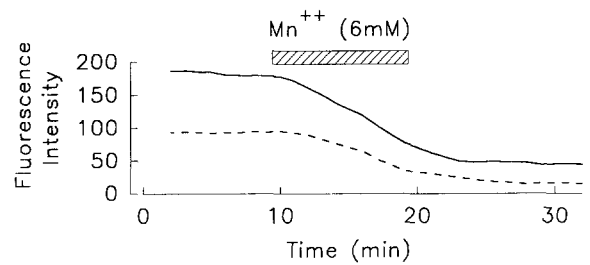


Fig. 7. Bath perfusion with 6 mM Mn^{++} results in fura 2 quenching and therefore a decrease in the fluorescence intensity at 340 nm (continuous line) and at 380 nm (broken line).

this cell type is similar to that in endothelial cells, then bath perfusion with Mn^{++} would decrease the fura 2 fluorescence intensity because fura 2 has a high affinity for Mn^{++} and is quenched upon binding. The effects of bath perfusion with Mn^{++} (5 mM) on the single wavelength fluorescence intensities are shown in Fig. 7. These results show that a Mn^{++} -permeable pathway is present in the plasma membrane of freshly dispersed rabbit corneal epithelial cells.

Discussion

Several types of Ca^{++} entry pathways have been characterized in nonexcitable cells. The mechanisms can be divided into four groups: voltage-gated calcium channels, nonselective divalent permeable cation channels, nonvoltage-gated calcium-selective channels, and exchange mechanisms such as Na^+ - Ca^{++} exchange. Chromaffin cells contain N-type (ω -conotoxin sensitive), P-type (ω -agatoxin sensitive), and dihydropyridine-sensitive calcium channels (Artalejo, Adams & Fox, 1994), which share the common feature of an increased open probability with membrane depolarization. A Mn^{++} and Ca^{++} permeable 2.5 pS nonvoltage-gated channel that is activated by inositol 1,3,4,5-tetrakisphosphate has been identified in cultured bovine endothelial cells (Luckhoff & Clapham, 1992). A different type of nonvoltage-gated calcium-selective conductance that is activated by internal calcium release has been identified in mast cells (Hoth & Penner, 1992). This particular calcium conductance is unusual in that it is not permeable to Mn^{++} , Sr^{++} , or Ba^{++} . Some nonselective cation channels are calcium permeable and thus represent a possible means for calcium influx. For example, in vascular endothelial cells a histamine-activated conductance shows a permeation ratio of 1:0.9:0.2 for K^+ : Na^+ : Ca^{++} and has a conductance of 8 pS in 110 mM Ca^{++} (Nilius, 1990). Finally, Na^+ - Ca^{++} exchange mechanisms may play a role in regulating cellular $[\text{Ca}^{++}]$ operating in forward mode, extruding Ca^{++} , or reverse mode thus contributing to Ca^{++} influx.

We have utilized single-cell fluorescence imaging technology with the ratiometric dye fura 2 to determine if the pathways described above may be involved in the regulation of Ca⁺⁺ entry, and therefore intracellular [Ca⁺⁺], in rabbit corneal epithelial cells. This study has shown that intracellular [Ca⁺⁺] is increased with membrane hyperpolarization and decreased with membrane depolarization. This pathway appears to be blocked by 5 mM Ni⁺⁺ and permeable to Mn⁺⁺. These results are consistent with a nonvoltage gated Ca⁺⁺ influx pathway, most similar to the pathway described in bovine endothelial cells (Luckhoff & Clapham, 1992). However, other mechanisms can't be ruled out. For example, a Ca⁺⁺ entry pathway that is activated by membrane hyperpolarization and inactivated by membrane depolarization, a Ca⁺⁺ permeable nonselective cation channel, or a Ca⁺⁺ exchange mechanism that is stimulated by membrane hyperpolarization would also be consistent with these results. ATP-dependent calcium transport, described in bovine corneal epithelial cells by Reinach et al. (1991), may be modulated by membrane potential (Ambudkar & Baum, 1988). They showed that the rate of Ca⁺⁺ uptake in vesicles was stimulated by a negative interior potential. Therefore, this mechanism would predict a decreased rate of Ca⁺⁺ efflux during membrane hyperpolarization, consistent with the experiments described here. Evidence supporting the presence of Na⁺-Ca⁺⁺ exchange was also obtained. Increasing intracellular [Na⁺] with ouabain and monensin followed by replacement of extracellular Na⁺ with Li⁺ resulted in an increase in intracellular [Ca⁺⁺], presumably resulting from Ca⁺⁺ influx via Na⁺-Ca⁺⁺ exchange operating in reverse mode. However, under physiological conditions this transport pathway would be expected to use the inwardly directed Na⁺ gradient for Ca⁺⁺ efflux.

The results also show that the magnitude of I_K may be modulated by intracellular [Ca⁺⁺]. Patch clamp experiments showed that stimulation by fenamates is less effective in Ca⁺⁺-free solutions when compared to normal Ringer's solution (containing 2.54 mM Ca⁺⁺). This result suggests that internal [Ca⁺⁺] plays a role in the regulation of I_K. Previous studies have alluded to this since external Ca⁺⁺ was required for stimulation of I_K with cGMP (Farrugia & Rae, 1992). Since flufenamic acid has been shown to increase activity of single channels in excised patches, stimulation of I_K is thought to partly result from a direct effect on the channel (Rae & Farrugia, 1992). The basis for the Ca⁺⁺-dependent component of stimulation of I_K is not clear. Previous studies have shown that I_K is not directly activated by alterations in [Ca⁺⁺]. Rather, the channel is partially blocked by Ca⁺⁺ at either face of the channel (Rae et al., 1990b). Therefore, the data suggest that the flufenamic acid-stimulated increase in internal [Ca⁺⁺] might initiate a signaling cascade that further activates I_K. We should note that maximum doses of flufenamic acid (500 μM)

were found to cause a rapid increase in intracellular [Ca⁺⁺], even in Ca⁺⁺-free bathing solutions, (*data not shown*) indicating that high doses of flufenamic acid elicit release of Ca⁺⁺ from internal stores. The point of convergence of this signal on the regulation of I_K is unclear at present.

It is interesting that a rise in internal Ca⁺⁺ is associated with an increase in I_K because this will, in turn, result in an increase in the driving force for Ca⁺⁺ entry thus providing a positive feedback mechanism. If the rise in [Ca⁺⁺] results from release from internal Ca⁺⁺ stores then this may represent a feedback mechanism allowing for efficient refilling of internal stores. Depletion of intracellular stores is accompanied by activation of Ca⁺⁺ influx due to release of an activating factor into the cytosol in many types of nonexcitable cells (Clapham, 1993; Neher, 1992). Further experiments will be necessary to determine if the calcium entry pathway is stimulated by depletion of intracellular Ca⁺⁺ stores, or if the increase in Ca⁺⁺ influx results solely from an increase in the driving force for Ca⁺⁺ entry.

The presented data are consistent with the hypothesis that the predominant mode for Ca⁺⁺ influx under physiological circumstances in rabbit corneal epithelial cells is via a nonvoltage-gated Ca⁺⁺ influx pathway. The conductance is Mn⁺⁺-permeable and is inhibited by Ni⁺⁺, which is similar to the Ca⁺⁺ influx pathway described in vascular endothelial cells (Luckhoff & Clapham, 1992). However, we should note that the data presented do not exclude a Ca⁺⁺ channel whose open probability increases with membrane hyperpolarization and decreases with membrane depolarization, or other Ca⁺⁺ transport mechanisms that are enhanced by membrane hyperpolarization, such as a Ca-ATPase. Electrophysiological experiments will be necessary to determine the precise molecular identity as well as the gating characteristics of this pathway. We have also presented data indicating the presence of Na⁺-Ca⁺⁺ exchange mechanisms in the plasma membrane, and we have shown that the magnitude of I_K is modulated by intracellular [Ca⁺⁺].

The authors are grateful to Chris Bartling for expert technical assistance with the imaging experiments, Helen Hendrickson for cell preparation, and Jonathon Monck for helpful discussions regarding imaging technology. This work was supported by National Institutes of Health grants EYO3282, EYO6005, DK08677, and an unrestricted award from Research to Prevent Blindness.

References

- Ambudkar, I.S., Baum, B.J. 1988. ATP-dependent calcium transport in rat parotid basolateral membrane vesicles is modulated by membrane potential. *J. Membrane Biol.* **102**:59-69
- Artalejo, C.R., Adams, M.E., Fox, A.P. 1994. Three types of Ca²⁺ channel trigger secretion with different efficacies in chromaffin cells. *Nature* **367**:72-76

- Clapham, D.E. 1993. A mysterious new influx factor? *Nature* **364**:763–764
- Farrugia, G., Rae, J.L. 1992. Regulation of a potassium-selective current in rabbit corneal epithelium by cyclic GMP, carbachol, and diltiazem. *J. Membrane Biol.* **129**:99–107
- Farrugia, G., Rae, J.L. 1993. Effect of volume changes on a potassium current in rabbit corneal epithelial cells. *Am. J. Physiol.* **264**:C1238–C1245, 1993
- Fasolato, C., Innocenti, B., Pozzan, T. 1994. Receptor-activated Ca²⁺ influx: how many mechanisms for how many channels? *Trends in Physiol. Sci.* **15**:77–83
- Grynkiewicz, G., Poenie, M., Tsien, R. 1985. A new generation of Ca²⁺ indicators with greatly improved fluorescence properties. *J. Biol. Chem.* **260**:3440–3450
- Hoth, M., Penner, R. 1992. Depletion of intracellular calcium stores activates a calcium current in rat mast cells. *Nature* **355**:353–355
- Luckhoff, A., Clapham, D.E. 1992. Inositol 1,3,4,5-tetrakisphosphate activates an endothelial Ca²⁺-permeable channel. *Nature* **355**:356–358
- Marks, P.W., Maxfield, F.R. 1991. Preparation of solutions with free calcium concentration in the nanomolar range using 1,2-Bis-(o-aminophenoxy)ethane-N,N,N',N'-tetraacetic acid. *Analytical Biochemistry* **193**:61–71
- Neher, E. 1992. Controls on calcium influx. *Nature* **355**:298–299
- Nilius, B. 1990. Permeation properties of a non-selective cation channel in human vascular endothelial cells. *Pfluegers Arch.* **416**:609–611
- Rae, J.L., Cooper, K., Gates, P., Watsky, M. 1991. Low access resistance perforated patch recordings using amphotericin B. *J. Neurosci. Methods* **37**:15–25
- Rae, J.L., Dewey, J., Cooper, K., Gates, P. 1990a. A non-selective cation channel in rabbit corneal endothelium activated by internal calcium and inhibited by internal ATP. *Exp. Eye Res.* **50**:373–384
- Rae, J.L., Dewey, J., Rae, J.S., Nesler, M., Cooper, K. 1990b. Single potassium channels in corneal epithelium. *Invest Ophthalmol. Vis. Sci.* **31**:1799–1809
- Rae, J.L., Farrugia, G. 1992. Whole-cell potassium current in rabbit corneal epithelium activated by fenamates. *J. Membrane Biol.* **129**:81–97
- Reinach, P.S., Holmberg, N., Chiesa, R. 1991. Identification of a calmodulin-sensitive Ca²⁺-transporting ATPase in the plasma membrane of bovine corneal epithelial cell. *Biochimica et Biophysica Acta* **1068**:1–8
- Reinach, P.S., Socci, R.R., Keith, C., Scanlon, M. 1992. Adrenergic receptor-mediated increase of intracellular Ca²⁺ concentration in isolated bovine corneal epithelial cells. *Comp. Biochem. Physiol.* **102A**:709–714
- Sage, S.O., van Breeman, C., Cannell, M.B. 1991. Sodium-calcium exchange in cultured bovine pulmonary artery endothelial cells. *J. Physiol.* **440**:569–580
- Schulze, D., Kofuji, P., Hadley, R., Kirby, M.S., Kieval, R.S., Doering, A., Niggli, E., Lederer, W.J. 1993. Sodium/calcium exchanger in heart muscle: molecular biology, cellular function, and its special role in excitation-contraction coupling. *Cardiovascular Research* **27**:1726–1734